Biomedical Optics EXPRESS

In vivo three-dimensional characterization of the adult zebrafish brain using a 1325 nm spectral-domain optical coherence tomography system with the 27 frame/s video rate

Jian Zhang, Wei Ge, and Zhen Yuan*

Faculty of Health Sciences, University of Macau, Taipa, Macau SAR, China
*zhenyuan@umac.mo

Abstract: In this study, a spectral-domain optical coherence tomography (SD-OCT) system was used for noninvasive imaging of the adult zebrafish brain. Based on a 1325 nm light source and two high-speed galvo mirrors, our SD-OCT system can offer a large field of view of brain morphology with high resolution (12 μm axial and 13 μm lateral) at video rate (27 frame/s). In vivo imaging of both the control and injured brain was performed using adult zebrafish model. The recovered results revealed that olfactory bulb, optic commissure, telencephalon, tectum opticum, cerebellum, medulla, preglomerular complex and posterior tuberculum could be clearly identified in the cross-sectional SD-OCT images of the adult zebrafish brain. The reconstructed results also suggested that SD-OCT can be used for diagnosis and monitoring of traumatic brain injury. In particular, we found the reconstructed volumetric SD-OCT images enable a comprehensive three-dimensional characterization of the control or injured brain in the intact zebrafish.

OCIS codes: (170.3880) Medical and biological imaging; (110.4500) Optical coherence tomography; (170.0110) Imaging systems

References and links

1. D. C. Lie, H. Song, S. A. Colamarino, G. L. Ming, and F. H. Gage, "Neurogenesis in the adult brain: new strategies for central nervous system diseases," Annu. Rev. Pharmacol. Toxicol. **44**(1), 399–421 (2004).
2. A. M. Siebel, A. L. Piato, K. M. Capiotti, K. J. Seibt, M. R. Bogo, and C. D. Bonan, "PTZ-induced seizures inhibit adenosine deamination in adult zebrafish brain membranes," Brain Res. Bull. **86**(5-6), 385–389 (2011).
3. N. Kyritsis, C. Kizil, S. Zocher, V. Kroehne, J. Kaslin, D. Freudenreich, A. Iltzsche, and M. Brand, "Acute inflammation initiates the regenerative response in the adult zebrafish brain," Science **338**(6112), 1353–1356 (2012).
4. O. Ronneberger, K. Liu, M. Rath, D. Rueß, T. Mueller, H. Skibbe, B. Drayer, T. Schmidt, A. Filippi, and R. Nitschke, "ViBE-Z: a framework for 3D virtual colocalization analysis in zebrafish larval brains," Nat. Methods **9**(7), 735–742 (2012).
5. F. Mahmood, S. Fu, J. Cooke, S. W. Wilson, J. D. Cooper, and C. Russell, "A zebrafish model of CLN2 disease is deficient in tripeptidyl peptidase 1 and displays progressive neurodegeneration accompanied by a reduction in proliferation," Brain **136**(5), 1488–1507 (2013).
6. Z. Yuan, "Combining independent component analysis and Granger causality to investigate brain network dynamics with fNIRS measurements," Biomed. Opt. Express **4**(11), 2629–2643 (2013).
7. Z. Yuan, J. Zhang, X. Wang, and C. Li, "A systematic investigation of reflectance diffuse optical tomography using nonlinear reconstruction methods and continuous wave measurements," Biomed. Opt. Express **5**(9), 3011–3022 (2014).
8. E. M. C. Hillman, "Optical brain imaging in vivo: techniques and applications from animal to man," J. Biomed. Opt. **12**(5), 051402 (2007).
9. G. Strangman, D. A. Boas, and J. P. Sutton, "Non-invasive neuroimaging using near-infrared light," Biol. Psychiatry **52**(7), 679–693 (2002).
10. M. B. Ahrens, M. B. Orger, D. N. Robson, J. M. Li, and P. J. Keller, "Whole-brain functional imaging at cellular resolution using light-sheet microscopy," Nat. Methods **10**(5), 413–420 (2013).

#240165 Received 4 May 2015; revised 4 Aug 2015; accepted 8 Sep 2015; published 11 Sep 2015

11. A. J. Giraldez, R. M. Cinalli, M. E. Glasner, A. J. Enright, J. M. Thomson, S. Baskerville, S. M. Hammond, D. P. Bartel, and A. F. Schier, "MicroRNAs regulate brain morphogenesis in zebrafish," Science **308**(5723), 833–838 (2005).
12. P. J. Keller, A. D. Schmidt, J. Wittbrodt, and E. H. K. Stelzer, "Reconstruction of Zebrafish Early Embryonic Development by Scanned Light Sheet Microscopy," Science **322**(5904), 1065–1069 (2008).
13. M. B. Ahrens, J. M. Li, M. B. Orger, D. N. Robson, A. F. Schier, F. Engert, and R. Portugues, "Brain-wide neuronal dynamics during motor adaptation in zebrafish," Nature **485**(7399), 471–477 (2012).
14. T. Mueller, M. F. Wullimann, and S. Guo, "Early teleostean basal ganglia development visualized by zebrafish Dlx2a, Lhx6, Lhx7, Tbr2 (eomesa), and GAD67 gene expression," J. Comp. Neurol. **507**(2), 1245–1257 (2008).
15. M. F. Wullimann and T. Mueller, "Teleostean and mammalian forebrains contrasted: evidence from genes to behavior," J. Comp. Neurol. **475**(2), 143–162 (2004).
16. S. Yun, G. Tearney, B. Bouma, B. Park, and J. de Boer, "High-speed spectral-domain optical coherence tomography at 1.3 μm wavelength," Opt. Express **11**(26), 3598–3604 (2003).
17. S. Hariri, M. Johnstone, Y. Jiang, S. Padilla, Z. Zhou, R. Reif, and R. K. Wang, "Platform to investigate aqueous outflow system structure and pressure-dependent motion using high-resolution spectral domain optical coherence tomography," J. Biomed. Opt. **19**(10), 106013 (2014).
18. Q. Zhang, M. Neitz, J. Neitz, and R. K. Wang, "Geographic mapping of choroidal thickness in myopic eyes using 1050-nm spectral domain optical coherence tomography," J. Innov. Opt. Heal. Sci. **8**, 1550012 (2014).
19. L. An, P. Li, T. T. Shen, and R. Wang, "High speed spectral domain optical coherence tomography for retinal imaging at 500,000 A-lines per second," Biomed. Opt. Express **2**(10), 2770–2783 (2011).
20. Z. Ma, A. Liu, X. Yin, A. Troyer, K. Thornburg, R. K. Wang, and S. Rugonyi, "Measurement of absolute blood flow velocity in outflow tract of HH18 chicken embryo based on 4D reconstruction using spectral domain optical coherence tomography," Biomed. Opt. Express **1**(3), 798–811 (2010).
21. L. Kagemann, H. Ishikawa, J. Zou, P. Charukamnoetkanok, G. Wollstein, K. A. Townsend, M. L. Gabriele, N. Bahary, X. Wei, J. G. Fujimoto, and J. S. Schuman, "Repeated, noninvasive, high resolution spectral domain optical coherence tomography imaging of zebrafish embryos," Mol. Vis. **14**, 2157–2170 (2008).
22. K. D. Rao, A. Alex, Y. Verma, S. Thampi, and P. K. Gupta, "Real-time in vivo imaging of adult zebrafish brain using optical coherence tomography," J. Biophotonics **2**(5), 288–291 (2009).
23. Y. S. Lin, C. C. Chu, P. H. Tsui, and C. C. Chang, "Evaluation of zebrafish brain development using optical coherence tomography," J. Biophotonics **6**(9), 668–678 (2013).
24. See supplementary material about the imaging-depth of our SD-OCT system.
25. Z. Zhang, B. Zhu, and W. Ge, "Genetic Analysis of Zebrafish Gonadotropin (FSH and LH) Functions by TALEN-Mediated Gene Disruption," Mol. Endocrinol. **29**(1), 76–98 (2015).
26. H. Grandel, J. Kaslin, J. Ganz, I. Wenzel, and M. Brand, "Neural stem cells and neurogenesis in the adult zebrafish brain: origin, proliferation dynamics, migration and cell fate," Dev. Biol. **295**(1), 263–277 (2006).
27. T. Mueller, "What is the thalamus in zebrafish?" Front. Neurosci. **6**, 64 (2012).
28. See supplementary material about the location of the imaging profile.

1. Introduction

The brain is the most complex organ which acts as the center of the nervous system. The brain is very vulnerable to central nervous system diseases including Alzheimer's disease, Parkinson's disease and multiple sclerosis [1]. The use of animal models in the field of basic neuroscience is able to significantly expand our knowledge in neurodegenerative diseases. In the last two decades, zebrafish has attracted much attention in the investigation of brain as a model organism of vertebrate biology [2–5]. This is largely due to the fact that the embryonic development of zebrafish is pretty rapid and the robust and transparent embryos has the capability to develop outside their mother.

As the gold standard, histological sectioning and staining are the most commonly used methods to investigate the internal structures of the zebrafish brain. However, these techniques need sacrifice the animals, which will bring significant challenges in studying the biological procedures in vivo and in dynamic processes. On the other hand, several optical imaging techniques including confocal and tow-photon microscopy have shown their advantages in imaging the zebrafish brain at embryonic stages [6–11]. The small volume and optical transparency for zebrafish brain at embryonic stages makes these optical imaging methods a perfect option to capture the brain structure and function in vivo [12, 13]. However, the widely used zebrafish strains will lose their transparency after their first two-week development. As a result, the most available optical imaging methods will not be able to effectively detect the zebrafish brain at juvenile or adult stages. Importantly, the change of brain structure and function as well as vertebrate neurogenesis appears not only during

#240165 Received 4 May 2015; revised 4 Aug 2015; accepted 8 Sep 2015; published 11 Sep 2015

embryonic stages, but also during juvenile or adult stages. For example, in the early zebrafish telencephalon, expression patterns of lim homeobox genes have shown that basal ganglia organization resembles that of mammals in the sense that pallidal primordium and striatal primordium are developed [14]. In contrast, in the adult teleost telencephalon, pallidal and striatal elements are found to be intermingled in the dorsal subpallium, in which separate pallidal or striatal components cannot be effectively characterized [15]. As such, it is crucial to develop and use new optical imaging techniques that are able to achieve a high-resolution characterization of the adult zebrafish brain in the large field of view in terms of good penetration depth, fast imaging speed and high imaging sensitivity.

Among all the available optical imaging methods, optical coherence tomography (OCT) is a well-developed technology that utilizes reflecting light to reconstruct the three-dimensional (3D) images of biological tissues with micrometer resolution. The latest generation OCT is SD-OCT, whose imaging speed is significantly improved by using spectrally separated detectors. In SD-OCT, the depth scan can be immediately implemented by Fourier-transform of the acquired spectra without the movement of the reference arm, which is able to result in fast imaging speed. Meanwhile the reduced losses during a single scan are capable of improving the signal to noise proportional to the number of detection elements. So far, SD-OCT has been widely used in the biological and biomedical imaging field [16–20]. Interestingly, OCT has been utilized to image the brain structures of zebrafish. However, most of the work was performed by using early-stage zebrafish [21]. More recently, two cases were reported that could capture part of the features of adult zebrafish brain based on OCT [22, 23]. However, due to the slow imaging speed and limited penetration depth, a comprehensive in vivo 3D characterization of the whole adult zebrafish brain has never been accomplished.

In this study, we employed a SD-OCT system for in vivo 3D imaging of the whole adult zebrafish brain, which can achieve noninvasive and fast neuroimaging at video rate without specific labeling. SD-OCT imaging was also implemented to show if it could reliably detect traumatic brain injury based on the zebrafish model. Interestingly it is observed from the imaging results that SD-OCT shows their promises for diagnosing traumatic brain injury and monitoring its progression. To the best of our knowledge, the complete brain structures from the adult zebrafish brain were depicted for the first time by using our SD-OCT systems.

2. Methods and materials

2.1 Experimental SD-OCT system

For our high performance SD-OCT system (TELESTO-II-1325LR, Thorlabs Inc., USA), the light source is a single superluminescent diode with 1325 nm central wavelength and over 100 nm spectral bandwidth. The SD-OCT system in Fig. 1 is able to achieve high resolution imaging (12 μm axial and 13 μm lateral resolution) at a longer imaging depth compared to previous OCT systems. The imaging depth of this system is ranged from ~6 mm in the agar phantom to ~2 mm in the tissues (chicken breast) as shown in Online Fig. 1 in the supplemental material [24]. Using two high-speed galvo mirrors, the SD-OCT enables rapid volume acquisitions at high imaging speed up to 76 kHz A-Scan per second, which can provide real-time, depth-resolved, cross sectional and 3D imaging. In this study, the resolution of a sagittal B-Scan is 1024 × 568 and we adopt 28 KHz scanning speed to obtain high quality SD-OCT images at video rate (27 frame/s). The maximum viewing field of this SD-OCT system can reach 16 × 16 mm. Data acquisition and imaging processing were simultaneity implemented with a high-performance computer.

#240165 Received 4 May 2015; revised 4 Aug 2015; accepted 8 Sep 2015; published 11 Sep 2015

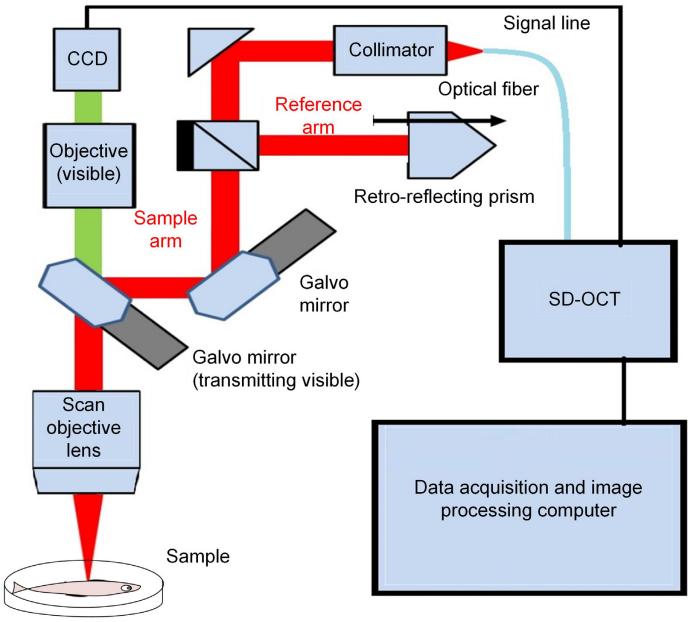

Fig. 1. Schematic of our SD-OCT system for imaging the adult zebrafish brain.

2.2 Experimental protocol

Wild type zebrafish of strain AB (n = 4, male, older than 90 days) were used in the present study. Zebrafish were maintained in our flow-through aquaria at temperature 28 ± 0.5 °C with the photo period of 14 hours light and 10 hours dark. All procedures were performed in compliance with the guidelines on animal research stipulated by the Animal Care and Use Committee at University of Macau. For imaging, the fish were first anaesthetized with 0.01% MS-222 in system water until they became unresponsive to touch [25]. Then the fish were moved to a petri dish containing two plexiglass panels that could keep the fish's body upright. Subsequently, the fish were placed in the field of view under the scan objective lens. After adjusting the focal plane to the suitable position upon the head of fish, we conducted both the cross-sectional and 3D imaging of adult zebrafish brain at video-rate imaging speed. Finally the data was processed to generate several sets of high-resolution 3D brain images.

For the investigation of surgery-induced brain injury, two wild type zebrafishes of strain AB (male, older than 90 days) were first anaesthetized and imaged before brain injury. Then a surgery was performed to use a sterile 25-gauge needle to cause a stab wound in the adult zebrafish brain. After half an hour, the zebrafishes were anaesthetized again and subsequently the injured brain was imaged by our SD-OCT system. Noted immediately after each of the experiments, these animals were put back into the fresh water.

3. Results and discussion

3.1 Cross-sectional SD-OCT imaging of the adult zebrafish brain

It is very important to conduct histological analysis of the adult zebrafish brain, which enable us to reveal its brain structures such as olfactory bulb, optic commissure, telencephalon, tectum opticum, cerebellum, medulla, preglomerular complex and posterior tuberculum [26]. Figure 2(a) was the schematic of the lateral view of adult zebrafish brain [27]. Based on the 1325 nm SD-OCT system, our findings showed that the morphology of the whole adult zebrafish brain and associated functional brain structures could be clearly identified in vivo in

#240165 Received 4 May 2015; revised 4 Aug 2015; accepted 8 Sep 2015; published 11 Sep 2015

the intact zebrafish. We firstly examined the brain images in Fig. 2(b) recovered by using the cross-sectional mode. It was observed from the sagittal SD-OCT images in Fig. 2(b) that we could effectively distinguish among the different functional structures of the adult zebrafish brain. Due to the difference of optical refractive index, the imaging intensity among the different structures recovered were also different. Interestingly it is noted from the imaging results in Fig. 2 that based on a 1325 nm low coherence light, the SD-OCT system was able to clearly identify the location of optic commissure, which is an important functional structure located at the very bottom of the adult zebrafish brain.

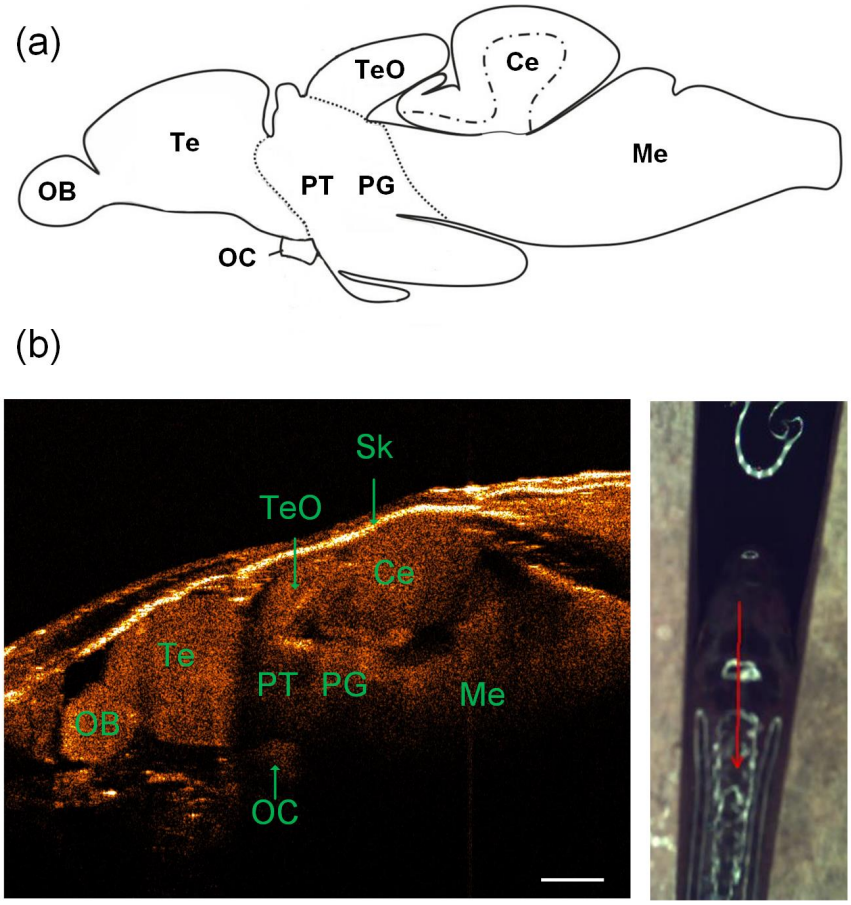

Fig. 2. (a) Schematic of the lateral view of adult zebrafish brain (the top row) [27]. (b) A representative sagittal SD-OCT image of the adult zebrafish brain (bottom left) along the red profile as shown in the photograph (bottom right): OB, olfactory bulb; OC, optic commissure; Te, telencephalon; TeO, tectum opticum; Ce, cerebellum; Me, medulla; PG, preglomerular complex; PT, posterior tuberculum; Sk, skull. The scale bar is 500 μm.

To demonstrate the morphology of the adult zebrafish brain in detail, coronal SD-OCT images were also reconstructed along four different profiles as plotted in Fig. 3. By accurately positioning the location of imaging profiles (Ref. 28), more specific information about the structures of the zebrafish brain were extracted from these images. We could see from these coronal SD-OCT images in Figs. 3(a)-3(d) that the whole zebrafish brain was reconstructed with a symmetric structure. For example, Fig. 3(a) plotted the coronal-section images of telencephalon, which has the shape of heart surrounded by bone. Figure 3(b) demonstrated that posterior tuberculum is the brain structure with relative low optical refractive index located between tectum opticum and optic commissure. In addition, it was observed from Fig.

#240165 Received 4 May 2015; revised 4 Aug 2015; accepted 8 Sep 2015; published 11 Sep 2015

3(c) that cerebellum is closely connected with preglomerular complex. Medulla and cerebellum are also identified by the coronal SD-OCT imaging, as displayed in Fig. 3(d).

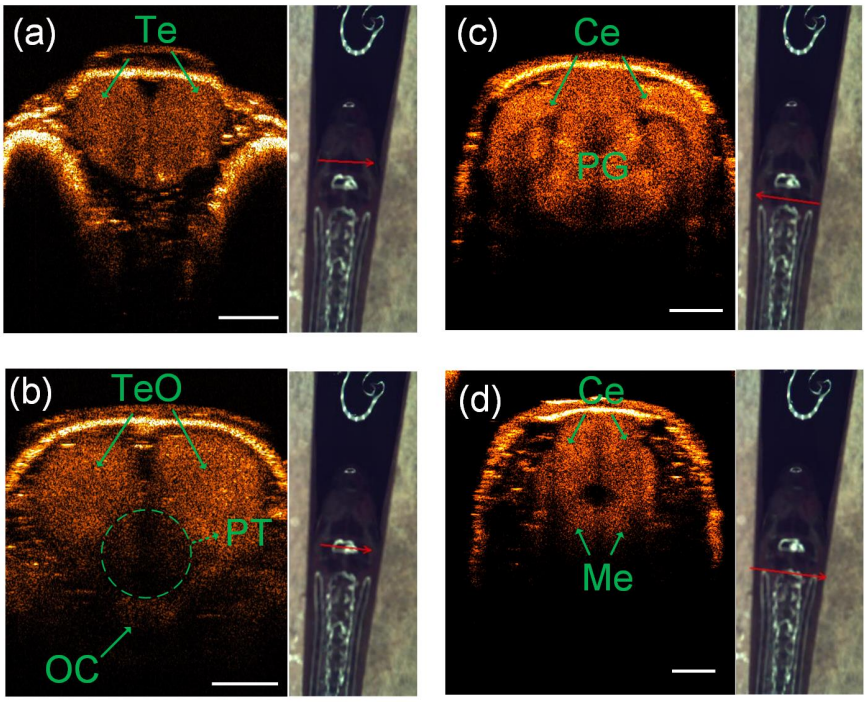

Fig. 3. Four different coronal SD-OCT images [(a) to (d)] at four different labeled positions on the head of the same adult zebrafish (see arrow locations and direction): OC, optic commissure; Te, telencephalon; TeO, tectum opticum; Ce, cerebellum; Me, medulla; PG, preglomerular complex; PT, posterior tuberculum. The scale bar is 500 μm.

3.2 3D SD-OCT imaging of the adult zebrafish brain

To show the whole 3D brain morphology, we performed the large field of view imaging of the adult zebrafish brain using our SD-OCT system, in which data was acquired at video-rate imaging speed. The region of interest (ROI, 5 × 2 mm) for imaging was located within the rectangle area as shown in Fig. 4(a), which could generate 263 sagittal SD-OCT images and could cover the whole head of the adult zebrafish. The imaging depth along the Z axis was set to 3 mm. Altogether 20 sagittal SD-OCT images of the adult zebrafish brain were generated and provided in Fig. 4(b). It was observed from the group of SD-OCT images that the brain morphology could be characterized and identified in detail. For example, the eye and other organs close to the zebrafish brain could be recovered with high resolution. The sliced SD-OCT images were then combined to form a 3D image, which could be displayed in the cross-sectional or volumetric form from a 3D view as shown in Fig. 5, Visualization 1 and Visualization 2.

#240165 Received 4 May 2015; revised 4 Aug 2015; accepted 8 Sep 2015; published 11 Sep 2015

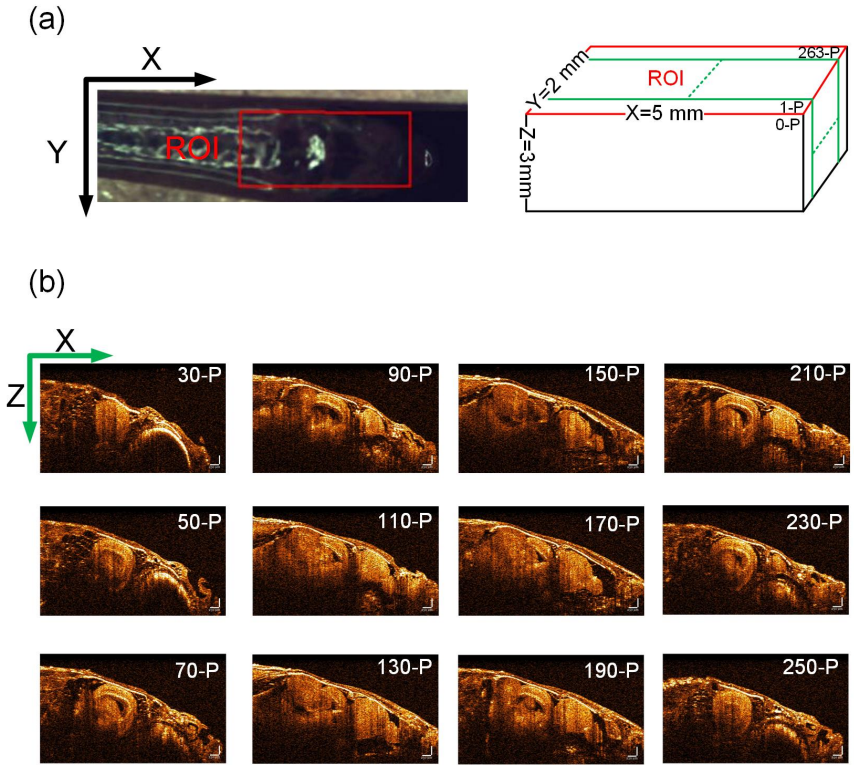

Fig. 4. (a) Region of interest (ROI) was labeled with a red rectangle in the photograph that could cover the whole brain. (b) Sequence of sagittal SD-OCT images of the adult zebrafish brain. The scale bar is 250 μm and is same for all the images.

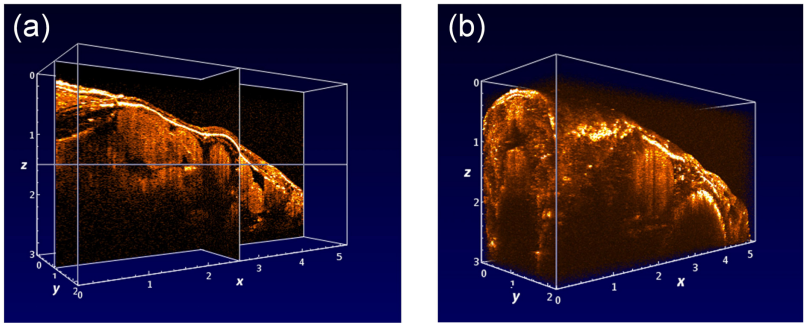

Fig. 5. 3D view of the reconstructed adult zebrafish brain in the cross-sectional form (a, Visualization 1) and volumetric form (b, Visualization 2).

3.3 Characterization of the adult zebrafish brain based-on the recovered 3D SD-OCT images

The best way to image the adult zebrafish brain by using SD-OCT is to keep zebrafish sample upright and then exam the brain from the top. Besides showing the brain structures from the sagittal view (X-Z) or coronal view (Y-Z) based on cross-sectional scanning, seven horizontal cross-sections at different depth were also extracted from the 3D SD-OCT images. With increased depths from 0.8 mm to 2.6 mm, we can see from Fig. 6 that the brain structures were clearly presented with high contrast and high resolution. The brain structures at each horizontal cross-section showed to have different imaging intensity, which is considered to be related to the optical refractive index of brain tissue. In addition, we also compared the reconstruction results from the horizontal section when z = 1.8 mm (Fig. 6) to those from the

#240165 Received 4 May 2015; revised 4 Aug 2015; accepted 8 Sep 2015; published 11 Sep 2015

coronal (Fig. 3(b)) and sagittal SD-OCT images (Fig. 2(b)). We found from the recovered images in Fig. 3 that the posterior tuberculum has relative low optical refractive index. These functional findings are crucial for functional brain imaging, which will be investigated in future. To the best of our knowledge, this is the first time to show that 3D SD-OCT enable a comprehensive characterization of the whole adult zebrafish brain from the horizontal view.

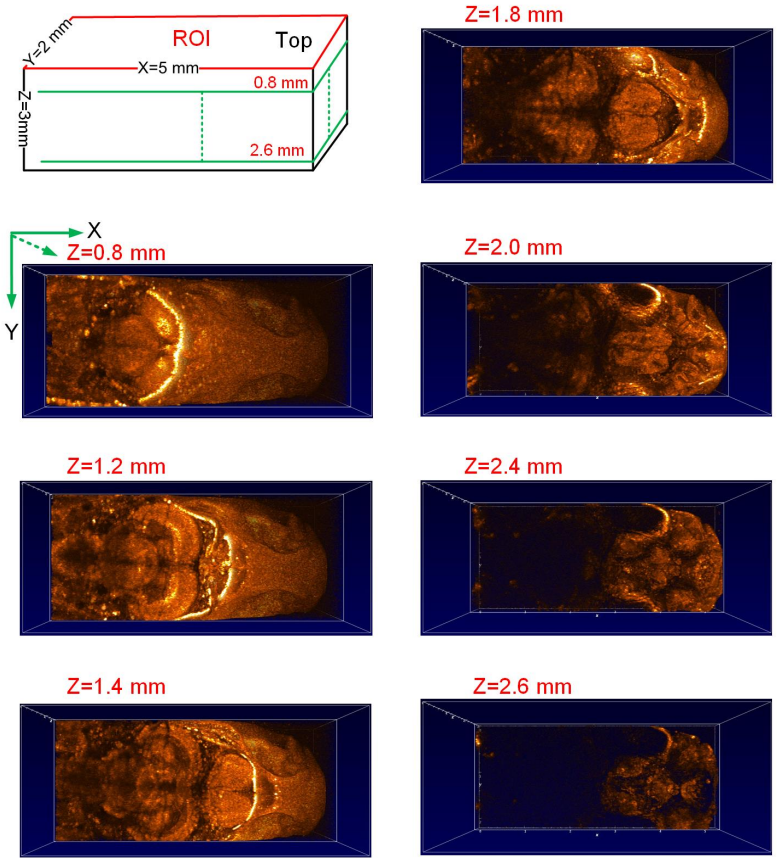

Fig. 6. Characterization of the adult zebrafish brain from the horizontal view based on the reconstructed 3D SD-OCT image of the same region of interest (ROI) as shown in Fig. 4 (a) with different imaging depths along Z axis with z = 0.8 mm, 1.2 mm, 1.4 mm, 1.8 mm, 2.0 mm, 2.4 mm and 2.6 mm, respectively.

3.4 Characterization of the injured adult zebrafish brain based-on the recovered 3D SD-OCT images

Additional tests were also implemented to see if SD-OCT can be used for diagnosis and monitoring of traumatic brain injury. Figure 7 showed the reconstructed results of the adult zebrafish in 3D brain before and after brain injury. Compared to the imaging results before brain injury, the injured areas on the skull labeled with blue dash lines and lesions inside the brain labeled with red dash lines were clearly identified. The 3D SD-OCT imaging enable a depth measurement of the lesion areas inside the brain tissues (~1.2 mm) as well as a diameter measurement of the wound along the skull (~0.3 mm). The horizontal images in Fig. 7 also revealed the position of the lesion was located in the center of the brain. Based on the recovered results from 3D SD-OCT imaging, we could see that the tectum opticum and posterior tuberculum were severely damaged after brain injury.

#240165 Received 4 May 2015; revised 4 Aug 2015; accepted 8 Sep 2015; published 11 Sep 2015

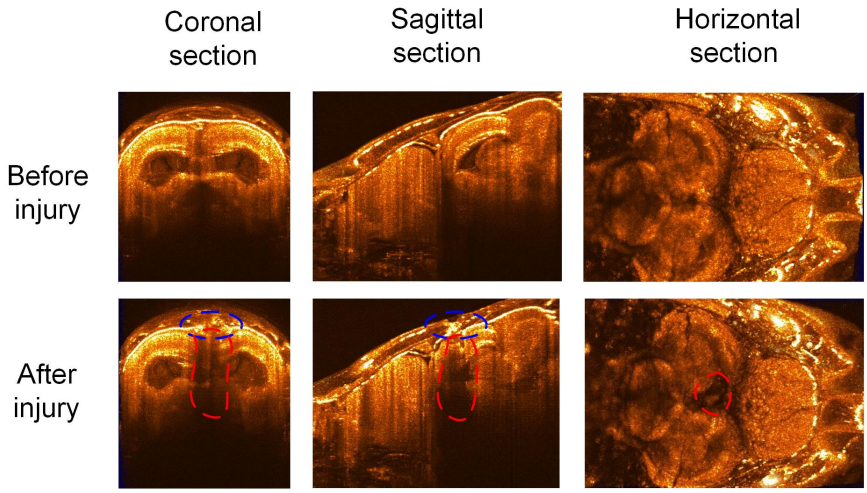

Fig. 7. Characterization of the adult zebrafish brain before (the first row) and after (the second row) brain injury. Columns one to three separately showed the coronal, sagittal and horizontal section of the 3D SD-OCT images.

4. Conclusion

In this study, the brain and associated functional structures of the adult zebrafish were in vivo characterized and identified by using our 1325 nm SD-OCT imaging system. The morphology and functional structures of the adult zebrafish brain could be clearly revealed from both the cross-sectional and 3D SD-OCT images. To the best of our knowledge, this the first time that the control and injured brain of the adult zebrafish were in vivo characterized and evaluated with a 3D SD-OCT imaging system. Importantly, our findings also suggested that SD-OCT shows its promise for zebrafish-based brain research in evolution, development and neuroscience.

Acknowledgments

Authors would like to thank Dr. Weiting Chen and Yuqin Fan for their help of raising zebrafish. This study was supported from University of Macau in Macau, SRG2013-00035-FHS Grant, MYRG2014-00093-FHS Grant, MYRG2015-00036-FHS grant and FDCT grant 026/2014/A1 from Macao government.